

Human cerebral venous outflow pathway depends on posture and central venous pressure

J. Gisolf¹, J. J. van Lieshout², K. van Heusden³, F. Pott⁴, W. J. Stok¹ and J. M. Karemaker¹

Departments of ¹Physiology and ²Internal Medicine, Academic Medical Center, Cardiovascular Research Institute Amsterdam, the Netherlands

³Systems and Control Group, Faculty of Mechanical Engineering, Delft University of Technology, the Netherlands

⁴The Copenhagen Muscle Research Center, Rigshospitalet, University of Copenhagen, Denmark

Internal jugular veins are the major cerebral venous outflow pathway in supine humans. In upright humans the positioning of these veins above heart level causes them to collapse. An alternative cerebral outflow pathway is the vertebral venous plexus. We set out to determine the effect of posture and central venous pressure (CVP) on the distribution of cerebral outflow over the internal jugular veins and the vertebral plexus, using a mathematical model. Input to the model was a data set of beat-to-beat cerebral blood flow velocity and CVP measurements in 10 healthy subjects, during baseline rest and a Valsalva manoeuvre in the supine and standing position. The model, consisting of 2 jugular veins, each a chain of 10 units containing nonlinear resistances and capacitors, and a vertebral plexus containing a resistance, showed blood flow mainly through the internal jugular veins in the supine position, but mainly through the vertebral plexus in the upright position. A Valsalva manoeuvre while standing completely re-opened the jugular veins. Results of ultrasound imaging of the right internal jugular vein cross-sectional area at the level of the laryngeal prominence in six healthy subjects, before and during a Valsalva manoeuvre in both body positions, correlate highly with model simulation of the jugular cross-sectional area ($R^2 = 0.97$). The results suggest that the cerebral venous flow distribution depends on posture and CVP: in supine humans the internal jugular veins are the primary pathway. The internal jugular veins are collapsed in the standing position and blood is shunted to an alternative venous pathway, but a marked increase in CVP while standing completely re-opens the jugular veins.

(Received 21 June 2004; accepted after revision 26 July 2004; first published online 29 July 2004)

Corresponding author J. Gisolf: Department of Physiology, Room M01-07, Academic Medical Center, University of Amsterdam, PO Box 22700, 1100 DE Amsterdam, the Netherlands. Email: j.gisolf@amc.uva.nl

In supine humans the internal jugular veins are the primary venous drain for the brain. In sitting and standing humans, however, the positioning of these veins above heart level causes them to collapse (Holt, 1941; Cirovic *et al.* 2003). A high outflow resistance would endanger cerebral blood flow in the upright posture if there were no alternative cerebral venous outflow pathway. There is an alternate pathway via the vertebral venous plexus (Batson, 1944; Zouaoui & Hidden, 1989; Chaynes *et al.* 1998) which extends from the intracranial venous sinuses to the superior caval system. Radiographic studies have shown the vertebral venous plexus to be the major exit pathway of cerebral blood in the erect position in Rhesus monkeys (Epstein *et al.* 1970). It was recently demonstrated that also in tree dwelling snakes, head-up tilt induces partial jugular collapse and shunting of cephalic blood flow into the vertebral plexus (Zippel *et al.* 2001). In sitting humans blood flow in the collapsed internal jugular veins is reported to be greatly reduced (Cirovic *et al.* 2003),

which together with evidence of an important role of the vertebral venous plexus in humans (Batson, 1940), suggests the pathway of the cerebral venous return to be posture dependent. Collapsed internal jugular veins can be completely reopened by positive pressure breathing in dogs (Toung *et al.* 2000) and in humans (Cirovic *et al.* 2003).

We developed a mathematical model of the cerebral venous outflow tract to study the distribution of cerebral blood flow to the internal jugular veins and to an alternative pathway (vertebral venous plexus). Input to the model are beat-to-beat measurements of central venous pressure (CVP) and cerebral blood flow velocity (CBFV), with and without an increased CVP by a Valsalva manoeuvre, in the supine and standing position. For the internal jugular veins we implemented a nonlinear pressure–volume relationship based on measurements by Braakman *et al.* (1989). Knowing the jugular veins to be collapsed in the upright position and re-opened during

positive pressure breathing, we hypothesized the cerebral outflow pathway to be dependent on posture and CVP. We expected the internal jugular veins to be the major drain for the brain in the supine position; in the standing position these veins are likely to be collapsed and to allow little blood flow. Furthermore we expected a 40 mmHg increase in CVP in the standing position to be sufficient to reopen the jugular veins and facilitate jugular blood flow for as long as CVP was raised. Ultrasound imaging of the internal jugular veins verified model outcome.

Methods

Model

To assess the cerebral venous outflow distribution over the internal jugular veins and the alternate pathway (the cervical vertebral venous plexus) we developed a beat-to-beat model programmed in Simulink of MATLAB (Release 5.2, The MathWorks, Natick, MA, USA). A detailed description of the mathematical model and a

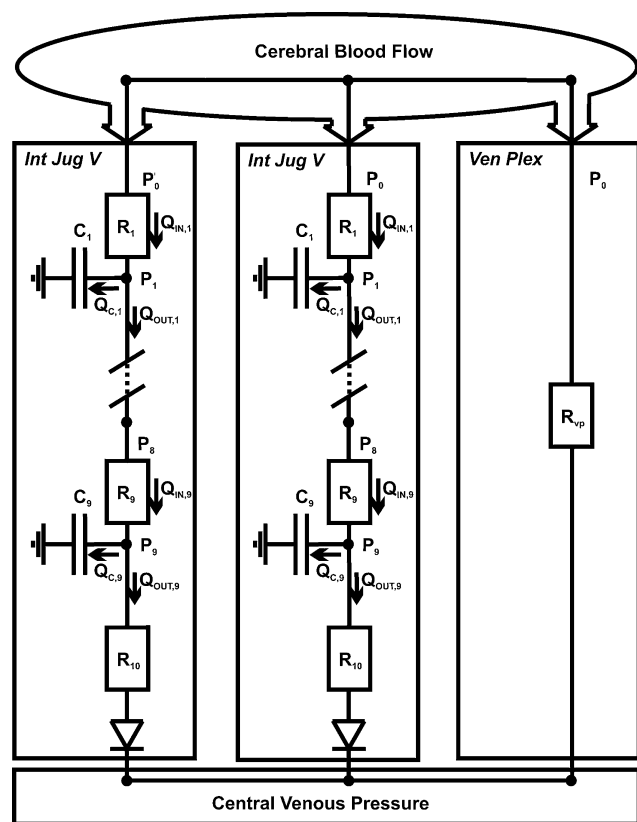


Figure 1. Schematic representation of the modelled cerebral venous outflow pathways

Int Jug V, internal jugular vein; Ven Plex, vertebral venous plexus; R_{vp} , venous plexus resistance. P_0 , pressure at the entrance and P_X , pressure at the exit of segment X . $R_{1...10}$, (variable) resistance of jugular segment 1...10 and $C_{1...9}$, (variable) capacity of jugular segment 1...9. $Q_{in,X}$, flow into segment X , $Q_{out,X}$, flow out of segment X , and $Q_{C,X}$, difference between the flow into and out of segment X .

parameter sensitivity analysis of the jugular vein model properties are given in the Appendix. Input data to the model are beat-to-beat measurements of CVP and CBFV variations. Lassen (1974) reported an average whole brain blood flow of $50 \text{ ml } (100 \text{ g})^{-1} \text{ min}^{-1}$ and considering a brain weight of 1500 g (Nelson, 1982), we assumed a supine cerebral blood flow of 750 ml min^{-1} for all subjects. CBFV (blood velocity rather than blood flow) was set to this level at baseline in the supine position and used to track variations in cerebral blood flow. A schematic representation of the modelled flow distribution to the internal jugular veins and the vertebral venous plexus is shown in Fig. 1. The blood flow out of the brain is assumed to be equal to the blood flow (velocity) into the brain as measured in the middle cerebral artery, as the brain has little pooling capacity (Monro-Kellie doctrine) (Kellie, 1822). Pulsatility is omitted by using the beat-averaged mean CBFV. Per heartbeat, the model computes the flow distribution over both jugular veins, which are modelled as being identical, and the vertebral venous plexus, which is modelled as an invariable resistance. To implement the effect of a hydrostatic pressure 'gradient' in the standing position, the model internal jugular vein was subdivided into a chain of 10 segments with a length of 1.5 cm each. The 9 most cranial segments each contain a variable resistor and capacitor, representing resistance to flow and the volume accommodating properties, respectively, while the most caudal segment contains a variable resistor but no capacitor (Fig. 1). In this caudal segment a jugular valve is implemented as a switch to a very high resistor (see Appendix), limiting flow reversal. The effects of gravity are implemented in the model as follows. The capacitance and resistance in each segment of the jugular veins are a function of the prevailing pressure in the segment (Braakman *et al.* 1989). The pressure-volume relation is highly nonlinear, with switch-like properties: at low (transmural) pressure, vessel volume is low; at high pressure the vessel volume approaches a maximal value (Fig. 2). In the standing position the pressure in each segment is corrected for hydrostatic pressure, and thus volume and resistance are computed from this level-corrected pressure. For example, in the standing position the most cranial part of the internal jugular vein is approximately 27 cm above heart level. This corresponds with a hydrostatic pressure correction of -21 mmHg . The height-corrected (low) transmural segment pressure will result in a low volume and a high resistance, in other words 'collapse' of the vessel, and subsequent shunting of blood to the venous plexus. Approximate venous plexus resistance is set at $0.068 \text{ mmHg s ml}^{-1}$ (as derived from previous studies, see Appendix). CVP measurements are input to the model; in the standing position a substantial increase in CVP, such as occurs during a Valsalva manoeuvre, will result in increased filling of the internal jugular veins.

Data set

The physiological data we used to test our model consist of CBFV (in the middle cerebral artery) and CVP measurements in 10 healthy young subjects (4 women, age 27 ± 6 years, height 180 ± 10 cm, weight 76 ± 10 kg) who participated in the study of Pott *et al.* (2000) for which informed consent had

been obtained from all participants, and which was approved by the ethics committee of Copenhagen (KF 01-120/96) and was performed in accordance with the guidelines laid down in the Declaration of Helsinki. The procedures are fully described elsewhere (Pott *et al.* 2000); summarizing, after instrumentation the subjects rested in the supine position for

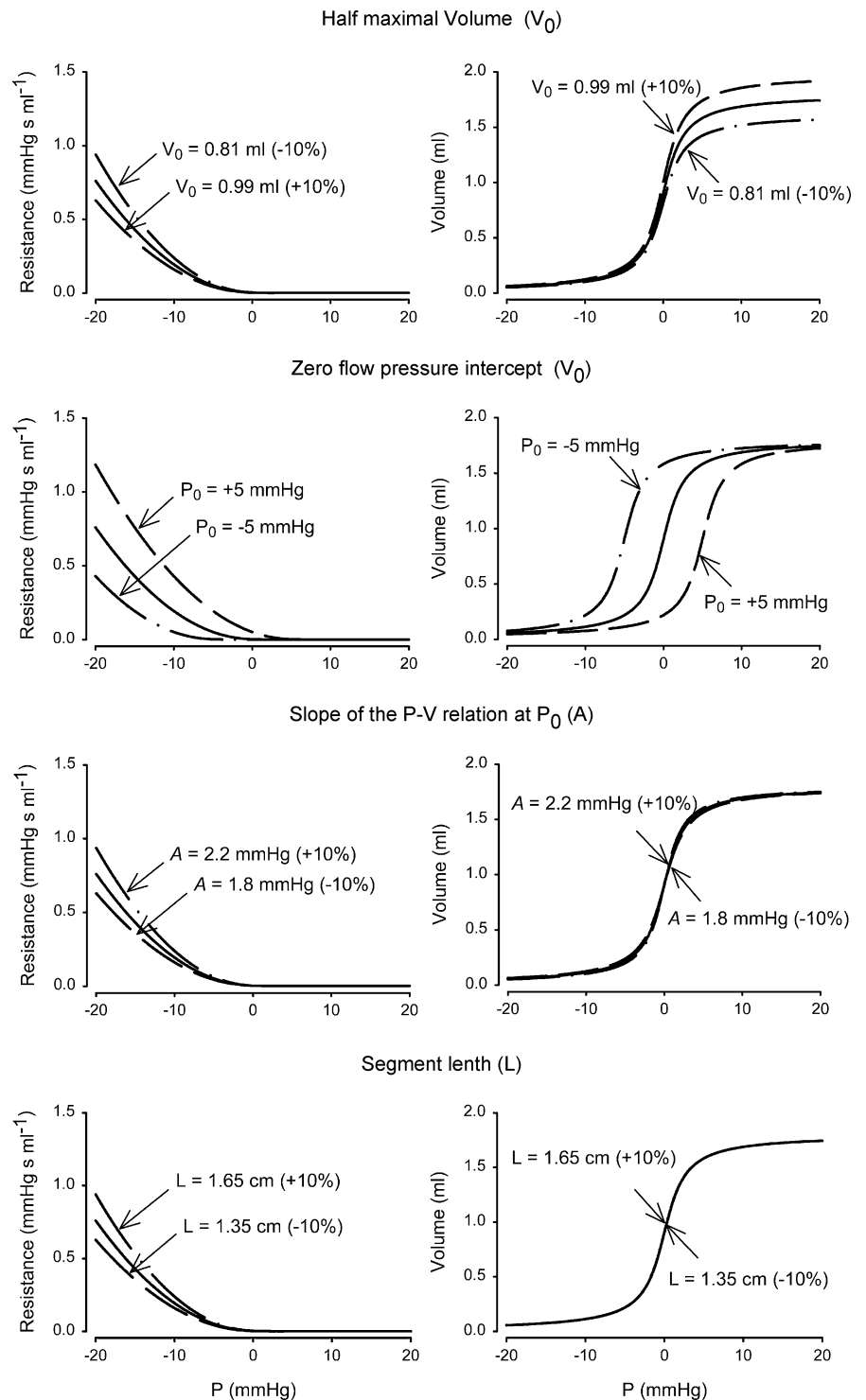


Figure 2. Parameter sensitivity analysis of variables used to model the pressure–volume and pressure–resistance relation in the internal jugular vein segments
 Equations of Braakman *et al.* (1989) are used. V_0 , half-maximal volume of the compartment; P_0 , zero flow pressure intercept; A , slope of P – V relation at V_0 ; L , length of the segment.

Table 1. Data set, model simulation and experimental results of supine and standing Valsalva manoeuvre

	Position	Phase			
		Baseline	IIa	IIb	IV
Data set*					
CVP (mmHg)	Supine	2 ± 1 [‡]	42 ± 4	44 ± 3	3 ± 1
	Standing	-2 ± 2 [‡]	40 ± 3	44 ± 4	-2 ± 2
CBFV (cm s ⁻¹)	Supine	76 ± 4 [‡]	62 ± 4	65 ± 4	79 ± 8
	Standing	66 ± 4 [‡]	55 ± 4	57 ± 4	71 ± 4
Model results*					
Int jug area (cm ²)	Supine	0.83 ± 0.09 [‡]	1.18 ± 0.002	1.18 ± 0.001	0.89 ± 0.08
	Standing	0.05 ± 0.01 [‡]	1.13 ± 0.03	1.15 ± 0.03	0.05 ± 0.01
Experiments[†]					
Int jug area (cm ²)	Supine	0.80 ± 0.11 [‡]	—	1.37 ± 0.28	—
	Standing	0.14 ± 0.03 [‡]	—	1.40 ± 0.29	—

Model results of the internal jugular vein area were derived from segment 5 (the middle segment); jugular vein echo images were taken at the level of the laryngeal prominence. Values are expressed as means ± s.e.m. CVP, central venous pressure; CBFV, cerebral blood flow velocity at the middle cerebral artery; Int jug area, cross-sectional area of the internal jugular vein. * Results from 10 subjects; † results from 6 subjects. ‡ Baseline differs from phase IIb of the Valsalva manoeuvre at the $P = 0.05$ level.

30 min. After a test run of a Valsalva manoeuvre, subjects rested for another 5 min and performed three Valsalva manoeuvres (40 mmHg expiratory pressure for 15 s), each followed by 3 min of recovery. Subjects were then asked to stand up in a relaxed position, and after 5 min they performed three Valsalva manoeuvres, each followed by 3 min of recovery. We analysed the first Valsalva in each body position.

The CBFV in the middle cerebral artery was measured using Transcranial Doppler (Multidop X, DWL, Sippligen, Germany). Mean CBFV was computed as the integral of the maximal frequency shifts over one beat divided by the corresponding beat interval. Finger arterial pressure was measured with a Finapres model 5 (Biomedical Instrumentation, TNO-BMI). For CVP measurement, a catheter (1.7 mm i.d., 16 gauge) was placed in the superior caval vein through the basilic vein. CVP was recorded from a transducer (Bentley, Uden, the Netherlands) fastened to the subject in the midaxillary line at the level of the right atrium and connected to a monitor (8041, Simonsen & Weel, Copenhagen, Denmark). Measurements were computed after analog to digital conversion at a sampling rate of 100 Hz. Finger arterial pressure, CVP and CBFV were averaged beat-to-beat, and CBFV was further processed to approximate variations in total cerebral blood flow.

Experiments

To verify the model outcome of internal jugular vein cross-sectional area before and during the straining phase of the Valsalva manoeuvre in the supine and standing position, the following protocol was carried

out in six healthy young subjects (3 women, age 31 ± 2 years, height 177 ± 3 cm, weight 70 ± 4 kg). Signed informed consent was obtained from all participants. The study was approved by the ethics committee of the Academic Medical Center (MEC 00/243) and performed in accordance with the guidelines laid down in the Declaration of Helsinki. Valsalva manoeuvres were conducted as described for 'Data Set'; this was practiced 1 day prior to the experiments. Subjects rested in the supine position for 5 min before they performed a Valsalva manoeuvre. They were then asked to stand up and remain standing for 5 min, and perform a Valsalva manoeuvre in the upright position. Upper arm blood pressure was measured at 2–3 min into the supine and upright periods (Omron M5-I, oscillometric blood pressure monitor).

The cross-sectional area of the right internal jugular vein was imaged using ultrasound (Acuson Aspen 7.0). The ultrasound probe was placed on the neck approximately at the level of the laryngeal prominence, so that the probe was perpendicular to the vessel and the location was marked. The imaging depth was 4 cm, and the gain 65 dB. To avoid compressing the vein, care was taken to exert minimal pressure with the probe. The image of the venous lumen was frozen on the screen of the ultrasound unit and saved on optical disk. The cross-sectional lumen area of the internal jugular vein was determined off-line from the ultrasound image. Ultrasound measurements were conducted 1 min prior to (baseline) and during the straining phase of the Valsalva manoeuvre (10 s from the start) in the supine and in the standing position. Where pulsations in the jugular vein were detected, the image at mid-point of the pulsation was stored.

Statistical analysis

Data are presented as means \pm s.e.m. Differences were tested by using paired *t* test; unequal variance (heteroscedastic) *t* test or sign test where appropriate. Pearson correlation coefficient was calculated for the correlation between the model estimates of the internal jugular vein cross-sectional areas and the ultrasound-determined areas. Group averages per event (baseline and Valsalva manoeuvre in the supine and standing position) were used. Significance was set at $P = 0.05$.

Results

Data set used for model simulation

The hemodynamic response to each Valsalva phase as defined from changes in blood pressure is described elsewhere (Pott *et al.* 2000); Table 1 gives the CVP and CBFV during baseline, phase IIa, IIb and IV. By definition (Sharpey-Schafer, 1965), in phase IIa (straining phase) of the Valsalva manoeuvre mean arterial pressure, pulse pressure and stroke volume decrease. This is followed by partial recovery of mean arterial pressure and heart

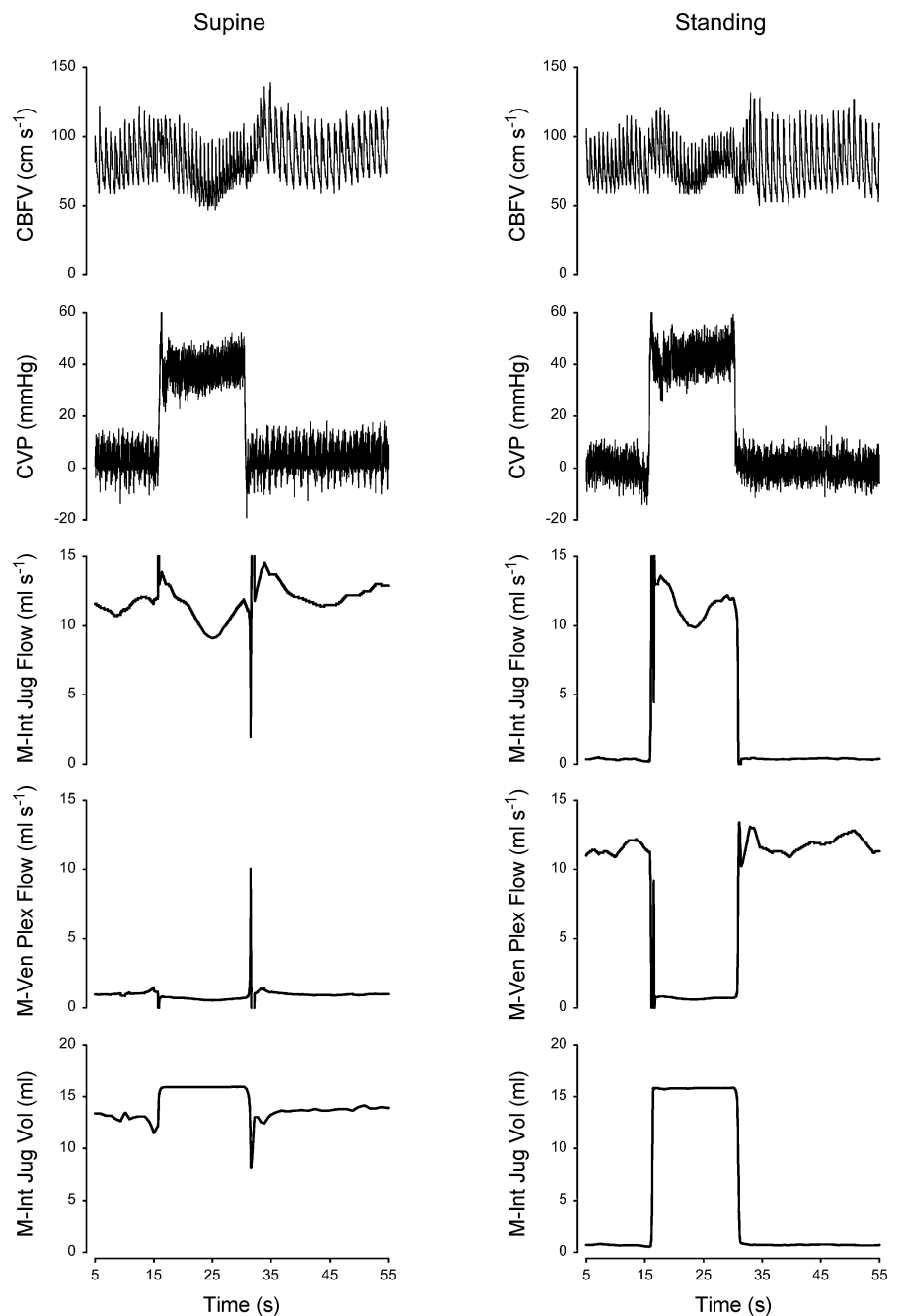


Figure 3. Cerebral venous outflow distribution during Valsalva manoeuvre in supine and standing position

Model simulation of cerebral outflow distribution and measurements of cerebral blood flow velocity (CBFV) and central venous pressure (CVP) in a subject who participated in the study of Pott *et al.* (2000). M-Int Jug Flow, flow into the internal jugular veins; M-Ven Plex Flow, vertebral venous plexus flow; M-Int Jug Vol, volume of each internal jugular vein.

rate toward the end of the strain, in phase IIb. Phase IV represents the arterial pressure overshoot after release of the strain. Cerebral venous outflow distribution over the internal jugular veins and the vertebral venous plexus was simulated using beat-to-beat variation in CVP and CBFV as input to the model (see Appendix for model description and settings). Figure 3 shows a representative example of CBFV and CVP measurements as well as simulated cerebral outflow distribution during supine and standing Valsalva manoeuvres; Fig. 4 shows simulation results averaged for all subjects.

Simulation of a supine Valsalva manoeuvre

Simulations of baseline flow and pressure in the supine position showed a cerebral venous outflow predominantly via the internal jugular veins (summed) and little flow via the vertebral venous plexus (Fig. 4). The pressure in the most cranial and most caudal jugular segments is given in Table 2; the pressure drop over the jugular veins in the supine position was only 0.2 mmHg. During phase IIb of the Valsalva manoeuvre, internal jugular vein volume and pressure increased ($P < 0.01$); the jugular veins remained the predominant cerebral outflow pathway.

Simulation of a standing Valsalva manoeuvre

Model simulation of baseline in the standing position showed a reduced internal jugular vein flow (Fig. 4; $P < 0.01$) and an increased venous plexus flow compared with supine baseline; the vertebral venous plexus was the main cerebral venous outflow pathway at baseline in the standing position. With a straining-induced increase in CVP (Valsalva), internal jugular vein volume and blood flow increased in phase IIb ($P < 0.01$ when compared with standing baseline); the jugular veins were the main cerebral venous outflow pathway during the straining phase of the Valsalva manoeuvre. Venous plexus blood flow decreased during straining in the standing position. Model estimates of the cross-sectional area of the internal jugular vein in the middle segment (Segment 5) during baseline and Valsalva manoeuvre phase IIa/b in the supine and standing position are given in Table 1.

Experiments

Upper arm arterial pressures, systolic and diastolic, were 120 ± 4 and 74 ± 1 mmHg, respectively, in the supine position and 120 ± 3 and 84 ± 3 mmHg, respectively, in the standing position. Table 1 gives the ultrasound-determined right internal jugular

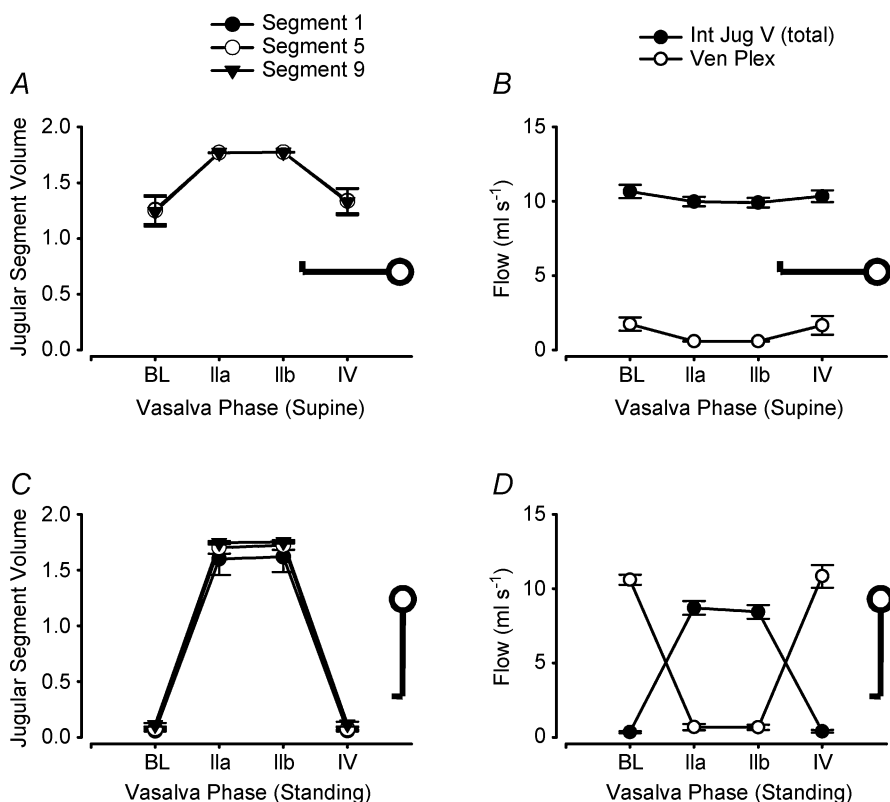


Figure 4. Simulation results of vertebral venous plexus flow and jugular segment flow and volume, in supine and standing Valsalva manoeuvres using an experimental data set of 10 healthy subjects

Symbols and error bars represent group means and s.e.m., respectively. BL, baseline; Int Jug V (total), internal jugular veins (total); Ven Plex, vertebral venous plexus.

Table 2. Model simulation of supine and standing Valsalva manoeuvre

Model results	Position	Phase	
		Baseline	IIb
Upper segment	Supine	2.7 ± 0.9 [‡]	44.2 ± 3.3
	Standing	-0.9 ± 2.1 [‡]	44.7 ± 3.6
Lower segment	Supine	2.5 ± 0.9 [‡]	44.2 ± 3.3
	Standing	-1.5 ± 2.1 [‡]	44.6 ± 3.6

Values are model internal jugular vein pressures (mmHg), uncorrected for height differences in the standing position. Simulation results from 10 subjects, expressed as means ± S.E.M.

[‡] Baseline differs from phase IIb of the Valsalva manoeuvre at the $P = 0.05$ level.

vein cross-sectional areas at the level of the laryngeal prominence. In the supine position the cross-sectional area was greater during a Valsalva manoeuvre compared with baseline ($P < 0.05$). In the standing position cross-sectional areas had diminished 6-fold, whereas a Valsalva manoeuvre while standing re-opened the vein (Fig. 5 shows a representative example). The ultrasound-determined right internal jugular veins areas, averaged per phase (baseline and 10 s from the start of a Valsalva manoeuvre approximating phase IIb) and per body position, correlated well with model predictions ($R^2 = 0.97$).

Discussion

The present study was designed to determine the effect of posture and CVP, on cerebral venous outflow distribution to the internal jugular veins and an alternative pathway, in humans. We developed a beat-to-beat mathematical model of two collapsible internal jugular veins and the vertebral venous plexus. Using measurements of CVP and variation in CBFV as input, model simulation of cerebral outflow distribution in the supine position indicated the internal jugular veins to be open, and to be the major outflow pathway. Raising CVP in the supine position further increased jugular vein volume. In the standing position, model simulation showed collapsed internal jugular veins at baseline, and opening of the jugular veins with increasing CVP. At standing baseline the cerebral outflow pathway was predominantly through the vertebral venous plexus, but this flow decreased with increasing CVP to be redirected through the internal jugular veins. Ultrasound imaging of internal jugular veins cross-sectional area during supine and standing Valsalva manoeuvres verified model outcome.

Collapsed internal jugular veins in upright humans imply an increased cerebral venous outflow resistance, and dependency on the vertebral venous plexus for cerebral venous return; this is illustrated in Fig. 6. During a Valsalva manoeuvre, elevation of CVP re-opens the jugular

veins, which implies a reduction of cerebral outflow resistance. The important implication is that everyday events involving straining, such as actively standing up, or coughing and sneezing, affect the cerebral outflow pathway and total outflow resistance. Evaluation of the total cerebral resistance is outside the scope of this study; for this, changes in intracranial pressure should be taken into account. The brain is enclosed in a rigid compartment and there is limited space for volume expansion; an increased tissue pressure may induce passive collapse of the (intracranial) venous outflow vessels with the development of a venous outflow resistance (Kongstad & Grände, 1999).

During the straining phase of the Valsalva manoeuvre in the standing position, model simulations indicate diminished vertebral venous plexus blood flow. Batson (1940) reported that flow in the vertebral venous plexus is actually reversed (directed in a caudal to cranial direction) during straining. He stated that vertebral plexus flow reversal during straining (such as induced by coughing) offered an explanation for the high incidence of cranial metastases with lung abscess and bronchiogenic carcinoma. He observed reversal of flow in the vertebral vein system with simulated abdominal straining in living monkeys, and reported that during the Valsalva manoeuvre blood is actually squeezed out of the intra-abdominal veins into the vertebral system, which is thought to contain no valves except in minor connecting channels. A more recent study by Chou *et al.* (2002) shows images of vertebral venous valves at the junction of the vertebral vein and the brachiocephalic vein. As our model does not demonstrate substantial vertebral plexus flow reversal, implementation of vertebral venous valves would not influence the simulations of flow distribution.

Incidentally, advances in high-resolution two- and three-dimensional computed tomography have allowed assessment of cranial venous outflow pattern in a very different subject group; this technique is used to assess endocranial capacity of remnants of the early hominids. An enlarged occipital-marginal sinus system in evolving bipedal hominids has been suggested to be related to factors involved with more efficient blood flow to the vertebral venous plexus (Conroy *et al.* 1990).

Model considerations and study limitations

The vertebral venous plexus is rudimentary in our model; it consists of a single non-varying resistance. Considering the multitude of anastomoses in this complicated network of plexus in humans, a more realistic approach would be a resistor and a capacitor with significant pooling properties. Adding a capacitor to the vertebral venous plexus in the model would result in charging of the capacitor during increased CVP, featuring caudal-to-cranial blood flow. The direction of flow

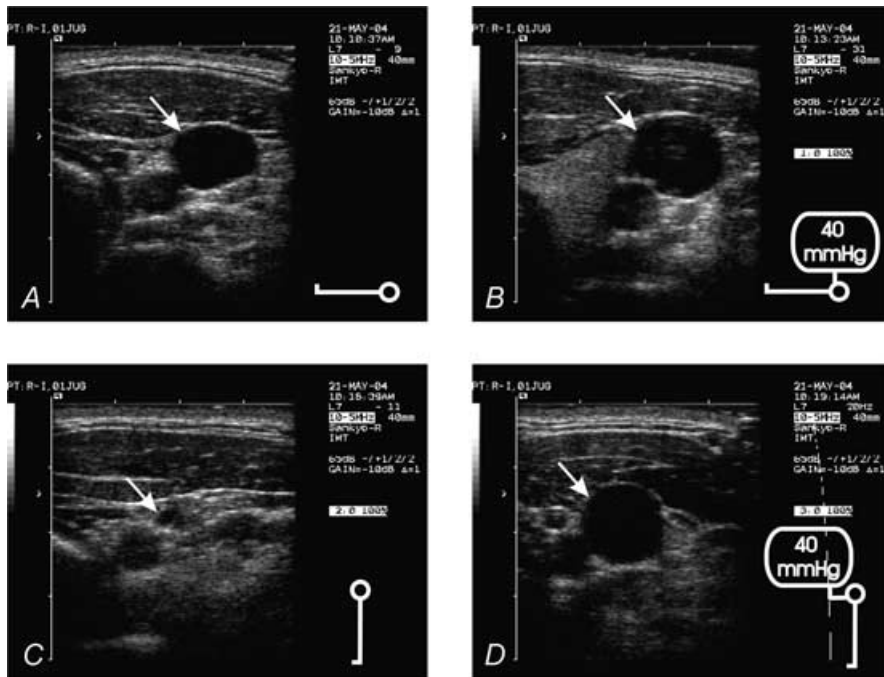


Figure 5. Ultrasound images of internal jugular vein lumen

The arrows indicate the right internal jugular vein lumen. *A*, subject is in the supine position, breathing normally; *B*, subject is in the supine position and performs a Valsalva manoeuvre; *C*, subject is standing, breathing normally; *D*, subject performs a Valsalva manoeuvre while standing.

would be determined by the placement of the capacitor; for example, significant extracranial venous pooling properties would result in caudal-to-cranial blood flow during straining. Although simplification of the venous plexus is a model limitation, the present study focuses on the effect of hydrostatics on internal jugular vein collapse and subsequent shunting of blood to the alternative pathway, and a rudimentary model seems sufficient to test our hypothesis. Further investigation into the vertebral venous plexus requires refinement of the model as well as venous plexus blood flow measurements.

The internal jugular veins are modelled as being identical. Asymmetry of the jugular veins volume under baseline conditions would result in unequal distribution of flow: a greater venous outflow through the larger jugular vein. The 'collapse pressure' of the veins would not be affected, however (see Appendix), and the overall distribution of jugular veins *vs.* alternative venous pathway would not be significantly altered. The nonlinear properties of the internal jugular veins are supported by a recent study addressing the absence of a siphon to support cerebral blood flow in standing humans (Dawson *et al.*

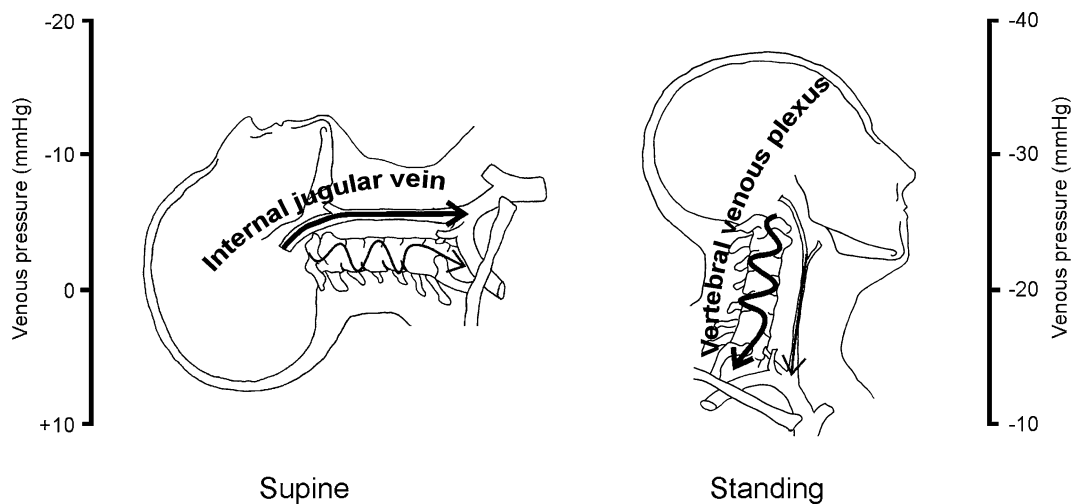


Figure 6. Illustration of the cerebral venous outflow pathways

Schematic representation of cerebral venous outflow pathway primarily via the internal jugular veins in the supine position (left) and the vertebral venous plexus in the upright position (right).

2004); collapse of jugular veins at tilt angles greater than 30–35° are reported. Valdueza *et al.* (2000) reported a large internal jugular flow decrease already at 15° tilt (from the horizontal position). A 10° head-down position increases internal jugular vein cross-sectional area (Schreiber *et al.* 2002).

For the individual model simulations, subject height was not taken into account. The rationale to take the distance from the heart to the internal jugular veins as equal for all subjects was the nonlinear characteristic of the veins: for a height difference of some 30 cm between subjects, the heart-to-neck distance might differ only a few centimetres. At a CVP of around zero at heart level, in the standing position the hydrostatic pressure correction at neck level will be sufficient to ensure collapse of the veins, irrespective of subject height.

Conclusions

In conclusion, in humans cerebral outflow pathways include internal jugular veins and an alternative route, the vertebral venous plexus system. Results of mathematical modelling suggest that whereas internal jugular veins are the major drain for the brain in the supine position, in the standing position they are liable to collapse and cerebral venous blood is returned via the alternative pathway. During increased CVP in the standing position the internal jugular veins are re-opened and these veins are again the primary pathway for cerebral venous return. Ultrasound images of the internal jugular vein cross-sectional area verify model outcome.

Appendix

Vertebral venous plexus resistance

The venous plexus resistance ($R_{\text{ven plex}}$) is indirectly derived from measurements by Cirovic *et al.* (2003). Using their measured jugular vein flow (Q_{jug}) and resistance (R_{jug}) in the supine and sitting position in the following equations:

$$Q_{\text{jug}}(\text{supine})R_{\text{jug}}(\text{supine}) = Q_{\text{ven plex}}(\text{supine})R_{\text{ven plex}}, \quad (\text{A1})$$

$$Q_{\text{jug}}(\text{sitting})R_{\text{jug}}(\text{sitting}) = Q_{\text{ven plex}}(\text{sitting})R_{\text{ven plex}}, \quad (\text{A2})$$

$$Q_{\text{jug}}(\text{sitting}) + Q_{\text{ven plex}}(\text{sitting}) = 0.9(Q_{\text{jug}}(\text{supine}) + Q_{\text{ven plex}}(\text{supine})), \quad (\text{A3})$$

where we take $R_{\text{ven plex}}$ as unvarying and Q_{jug} as the flow through the internal jugular veins. $Q_{\text{ven plex}}$ represents the flow through the vertebral venous plexus. Assuming the total cerebral flow in the sitting position to be 90% of the flow in the supine position, and filling in $Q_{\text{jug}}(\text{supine}) = 931 \text{ cm}^3 \text{ min}^{-1}$;

$R_{\text{jug}}(\text{supine}) = 0.13 \text{ mmHg min cm}^{-3}$; $Q_{\text{jug}}(\text{sitting}) = 372 \text{ cm}^3 \text{ min}^{-1}$; $R_{\text{jug}}(\text{sitting}) = 6.3 \text{ mmHg min cm}^{-3}$, brings us to a $R_{\text{ven plex}}$ (scaled to a cerebral blood flow level of 12.5 ml s^{-1} in the supine position) of $0.068 \text{ mmHg s ml}^{-1}$.

Model equations

The structure of the cerebral venous outflow model is shown in Fig. 1. Inputs to the model are central venous pressure (CVP) and variations in cerebral blood flow (CBFV), which is computed by scaling beat-to-beat cerebral blood flow velocity (CBFV) data to a physiological range as described in the Methods section. Extra-vascular pressure in the neck is assumed to be atmospheric pressure. CBFV is distributed over two identical jugular veins and the cervical vertebral venous plexus.

Flow through the venous plexus is computed from the resistance in the venous plexus, the pressure at the beginning of the cerebral outflow tract (P) and the central venous pressure:

$$Q_{\text{ven plex}} = (P - \text{CVP})/R_{\text{ven plex}}, \quad (\text{A4})$$

where $R_{\text{ven plex}}$ is set at $0.068 \text{ mmHg s ml}^{-1}$. Consequently, the blood flow into the jugular veins is the total CBFV minus the venous plexus blood flow.

The jugular vein is arbitrarily divided into 10 segments of equal length. Nine segments consist of a variable resistor and capacitor (Fig. 1), while the most caudal segment consists of a resistor only. For each segment X of the jugular vein, where $X = 1$ is the most cranial and $X = 10$ the most caudal segment, the hydrostatic pressure correction can be calculated as ρgh_X , where h_X is the height difference between segment X and the heart, ρ is the density of blood and g is the gravitational acceleration. The height-corrected pressure (P_{HC}) is only used for calculation of the resistance (R_X), capacity (C_X) and volume (V_X) of each segment (eqns A5–7) using equations presented by Braakman *et al.* (1989) as illustrated in Fig. 2:

$$R_X(P_{\text{HC}}) = (8\eta\pi L^3)/(V_0(1 + (2/\pi(\text{atan}((P_{\text{HC}} - P_0)/(A))))))^2 \quad (\text{A5})$$

$$C_X(P_{\text{HC}}) = 2V_0/(\pi A(1 + ((P_{\text{HC}} - P_0)/(A)^2))) \quad (\text{A6})$$

$$V_X(P_{\text{HC}}) = V_0(1 + 2/\pi(\text{atan}((P_{\text{HC}} - P_0)/(A)))) \quad (\text{A7})$$

where L is the length of the segment, η is the viscosity of blood, P_0 and V_0 are parameters related to vascular tone and volume range, respectively, and A is the slope of the P - V relation at V_0 .

Table 3. List of definitions

Symbol	Definition	Unit	Type	Value
A	Slope of P - V relation at V_0	mmHg	Parameter	2
$CBFV$	Cerebral blood flow velocity	cm s^{-1}	Data set	—
$CBFV$	Cerebral blood flow velocity, set to a physiological range	ml s^{-1}	Data input	—
CVP	Central venous pressure	mmHg	Data input	—
C_X	Compliance in jugular segment X	ml mmHg^{-1}	Computed	—
g	Gravitational acceleration	m s^{-2}	Parameter	9.8
h_X	Height distance from the heart	cm	Parameter	$12 < h_X < 27$
L	Segment length	cm	Parameter	1.5
P	Pressure before the outflow tract	mmHg	Computed	—
P_0	Zero flow pressure intercept	mmHg	Parameter	0
P_{HC}	Height-corrected pressure	mmHg	Computed	—
P_X	Pressure in segment X	mmHg	Computed	—
$Q_{C,X}$	Net flow into segment X	ml s^{-1}	Computed	—
$Q_{in,X}$	Flow into segment X	ml s^{-1}	Computed	—
Q_{jug}	Jugular blood flow	ml s^{-1}	Computed	—
$Q_{out,X}$	Flow out of segment X	ml s^{-1}	Computed	—
$Q_{ven\ plex}$	Vertebral cervical venous plexus	ml s^{-1}	Computed	—
$R_{ven\ plex}$	Resistance in the venous plexus	mmHg s ml^{-1}	Parameter	0.068
R_X	Resistance in jugular segment X	mmHg s ml^{-1}	Computed	—
V_0	Half-maximal segment volume	cm^3	Parameter	0.9
V_X	Volume in jugular segment X	cm^3	Computed	—
η	Viscosity of blood	mmHg s^{-1}	Parameter	2.9×10^{-5}
ρ	Density of blood	kg m^{-3}	Parameter	1.05×10^3

The blood flow out of segment X ($Q_{out,X}$) is computed from the inflow ($Q_{in,X}$) and the volume change (dV_X/dt):

$$Q_{out} = Q_{in} - dV_X/dt \quad (\text{A8})$$

The blood flow into the most cranial segment ($X = 1$) is Q_{jug} .

The pressure (non-height corrected) before the resistance of each segment, P_{X-1} (Fig. 1), is calculated from Q_{in} , R_X and the pressure (P_X) after the resistance:

$$P_{X-1} = P_X + Q_{in,X} R_X \quad (\text{A9})$$

The pressure after the resistance in the most caudal compartment $X = 10$, is the CVP, which is input to the model. When CVP exceeds the pressure in compartment $X = 9$, the most caudal compartment's resistance (R_{10}) switches from a resistance modelled as equal to the resistance in R_9 , to a high invariable resistance of $100 \text{ mmHg s ml}^{-1}$, which is how the jugular valves are implemented in the model.

Parameter sensitivity analysis

To determine the sensitivity of the model to the input variables, we computed the pressure–volume and the pressure–resistance relation using the input variables as were used for the model simulations, and by varying the parameters determining the pressure–volume relation by 10%. For P_0 , the zero-flow pressure intercept, which

was set at 0, we computed -5 and $+5$ mmHg as well as 0. The results are shown in Fig. 2, where the resistance and volume are those in a jugular vein segment, as a function of the height-corrected pressure in the segment. The figure illustrates that P_0 determines the volume of the vein segment at a certain segment pressure. This pressure is uncorrected for pressure in the neck; neck-suction for example will decrease the surrounding pressure in the neck, and the pressure in the segment can be corrected to obtain transmural pressure. Figure 2 also shows the influence of hydrostatic pressure differences. In transition from supine to standing, the reduction in segment pressure due to hydrostatics greatly influences the volume and resistance of the segment at pressures below 0; at high (central venous) pressure, such as occurs during straining, the height-corrected pressure in the vessel will be in the positive range regardless of posture.

References

- Batson OV (1940). The function of the vertebral veins and their role in the spread of metastases. *Ann Surg* **112**, 138–149.
- Batson OV (1944). Anatomical problems concerned in the study of cerebral blood flow. *Fed Proc* **3**, 139–144.
- Braakman R, Sipkema P & Westerhof N (1989). A dynamic nonlinear lumped parameter model for skeletal muscle circulation. *Ann Biomed Eng* **17**, 593–616.
- Chaynes P, Verdier JC, Moscovici J, Zadeh J, Vaysse P & Becue J (1998). Microsurgical anatomy of the internal vertebral venous plexuses. *Surg Radiol Anat* **20**, 47–51.

- Chou CH, Chao AC & Hu HH (2002). Ultrasonographic evaluation of vertebral venous valves. *AJNR Am J Neuroradiol* **23**, 1418–1420.
- Cirovic S, Walsh C, Fraser WD & Gulino A (2003). The effect of posture and positive pressure breathing on the hemodynamics of the internal jugular vein. *Aviat Space Environ Med* **74**, 125–131.
- Conroy GC, Vannier MW & Tobias PV (1990). Endocranial features of *Australopithecus africanus* revealed by 2- and 3-D computed tomography. *Science* **247**, 838–841.
- Dawson EA, Secher NH, Dalsgaard MK, Ogoh S, Yoshiga CC, Gonzalez-Alonso J, Steensberg A & Raven PB (2004). Standing up to the challenge of standing: a siphon does not support cerebral blood flow in humans. *Am J Physiol Regul Integr Comp Physiol* (ahead of print).
- Epstein HM, Linde HW, Crampton AR, Ciric IS & Eckenhoff JE (1970). The vertebral venous plexus as a major cerebral venous outflow tract. *Anesthesiology* **32**, 332–337.
- Holt JP (1941). The collapse factor in the measurement of venous pressure. *Am J Physiol* **134**, 292–299.
- Kellie G (1822). On death from cold, and on congestion of the brain. *Transactions Med-Chirurg Soc Edinburgh* **1**, 84–169.
- Kongstad L & Grände PO (1999). The role of arterial and venous pressure for Volume regulation of an organ enclosed in a rigid compartment with application to the injured brain. *Acta Anaesthesiol Scand* **43**, 501–508.
- Lassen NA (1974). Control of cerebral circulation in health and disease. *Circ Res* **34**, 749–760.
- Nelson GE (1982). *Fundamental Concepts of Biology*. New York: Wiley, p. 262.
- Pott F, van Lieshout JJ, Ide K, Madsen P & Secher NH (2000). Middle cerebral artery blood velocity during a valsalva maneuver in the standing position. *J Appl Physiol* **88**, 1545–1550.
- Schreiber SJ, Lambert UK, Doepp F & Valdueza JM (2002). Effects of prolonged head-down tilt on internal jugular vein cross-sectional area. *Br J Anaesth* **89**, 769–771.
- Sharpey-Schafer EP (1965). Effect of respiratory acts on the circulation. In *Handbook of Physiology. Circulation*. Sect. 2, Vol. III. Chapt. 52, pp. 1875–1886. Washington, DC.
- Toung TJK, Aizawa H & Traystman RJ (2000). Effects of positive end-expiratory pressure ventilation on cerebral venous pressure with head elevation in dogs. *J Appl Physiol* **88**, 655–661.
- Valdueza JM, von Munster T, Hoffman O, Schreiber S & Einhaupl KM (2000). Postural dependency of the cerebral venous outflow. *Lancet* **355**, 200–201.
- Zippel KC, Lillywhite HB & Mladinich CR (2001). New vascular system in reptiles: anatomy and postural hemodynamics of the vertebral venous plexus in snakes. *J Morph* **250**, 173–184.
- Zouaoui A & Hidden G (1989). The cervical vertebral venous plexus, a drainage route for the brain. *Surg Radiol Anat* **11**, 79–80.

Acknowledgements

This study was supported by a grant from the Space Research Organization Netherlands (SRON), project MG-052. The authors thank J. Gort and W. Hanselaar for the ultrasound imaging. We appreciate J.O. Fortrat's introduction to the hominid evolution through bipedalism.